Journal of Sound and Vibration (1998) **214**(2), 339–357
Article No. sv981587

A METHOD TO IDENTIFY MODAL PARAMETERS AND GEAR ERRORS BY VIBRATIONS OF A SPUR GEAR PAIR

M. Amabili

Dipartimento di Ingegneria Industriale, *Università di Parma*, *I*-43100 *Parma*, *Italy*

AND

A. Fregolent

Dipartimento di Meccanica ed Aeronautica, *Università di Roma "La Sapienza"*, *I*-00184 *Roma*, *Italy*

(*Received* 10 *February* 1997, *and in final form* 19 *February* 1998)

A new method to identify modal parameters (natural frequency and damping) and the equivalent gear error of a spur gear pair is introduced. The equivalent error is a function of the gear position and is related to the errors of the driving and the driven gears and to the non-dimensional stiffness of the teeth. The method is based on the measurement of the gear torsional vibrations. The test rig is modelled as a single-degree-of-freedom system and must be assembled by using stiff bearings and torsionally compliant shafts. The solution of the equation of motion is obtained through the harmonic balance method. The proposed approach has some advantages with respect to traditional metrological methods. The effect of noise on the accuracy of the identification is also investigated and discussed. Applications of the method to the identification of natural frequency, damping and profile errors are shown.

1. INTRODUCTION

Many papers have been published in the past 15 years on the effect of gear errors on the dynamic response of gear pairs, e.g. references [1–16]. Vibrations of gear pairs are largely affected by the amplitude and phase of deviations of the tooth profile from the true involute one. Pitch, pressure angle and mounting (eccentricities and misalignments) errors are also of great importance. As a result, gear errors must be checked in order to avoid bad working conditions of high-speed gears and silent reducers. In addition, profile modifications are introduced to reduce gear vibrations, therefore, their accuracy and efficacy must be verified. Analytical [3, 14, 17–20], numerical [2, 9–13, 15, 21–26] and approximate [6] methods were proposed in the past to simulate the dynamics of a spur gear pair, and single [2, 3, 5–12, 23, 24], multi [4, 20, 25–27] or infinite [28] degrees of freedom were used by different authors to model the system's behaviours. Multi axes reducers were also investigated e.g. in references [13, 14].

An extended review of the literature on gear dynamics is presented by Özgüven and Houser [1] and a review of the theory and experimental measurement of gear transmission error is given by Munro [29]. In the present work, references [2, 3, 5, 6, 10] are extensively used. Özgüven and Houser [2] used a single-degree-of-freedom model that includes the effects of variable mesh stiffness, damping, gear errors, profile modifications and backlash.

0022–460X/98/270339 + 19 $30.00/0

Amabili and Rivola [3] included the effect of time-varying meshing damping; in this case the solution is obtained by using the harmonic balance method. Cai and Hayashi [5] proposed a method to calculate the optimum profile modification in order to obtain a zero vibration of the gear pair. They also proposed [6] a linear approximate equation to model the gear pair by using a single-degree-of-freedom model. Experimental results were obtained by using a sophisticated test rig with high stiffness air bearings specifically designed for this application. Umezawa *et al*. [10] also used a single-degree-of-freedom numerical simulation, the results of which are compared with experimental dynamic transmission errors obtained for a gear pair having unit gear ratio.

In the present study, a method based on the measurement of the gear torsional vibrations is proposed to identify the natural frequency and the damping of the system and to evaluate the equivalent gear error of a spur gear pair. The equivalent error is a function of the gear position having length as its dimension. It is related to the errors of the driving and the driven gears and to the non-dimensional stiffness of the teeth. The system is analytically studied by using a single-degree-of-freedom system capable of modelling the experimental test rig. This must be assembled using stiff bearings and torsionally compliant shafts. However, the shafts must be stiff with respect to flexion at the gears' position. In fact, this design criterion ensures a good approximation to uncouple the torsional vibrations of the two gears due to mesh stiffness from the other modes of the test rig. This kind of apparatus was recently assembled, e.g., by Cai and Hayashi [6] and Blankenship and Kahraman [30, 31]. If gear pairs have different centre distances, an appropriate housing or different housings must be built.

The solution of the equation of motion is obtained through the harmonic balance method [32]. This solution is suitable to model spur gear pairs having low contact ratio ε (i.e., $1 < \varepsilon < 2$) and to identify pitch, profile, pressure angle and runout errors. Results can be obtained by using an experimental apparatus requiring only the measurement of vibration response of the driven gear (or driving and driven gears) during a revolution for at least three different rotational speeds. The gear pair must be tested with a fixed static load. In the case of testing a single gear, this one must be coupled with a reference.

Calculation and experimental identification of the natural frequency and damping of a gear pair is still far from being considered as well established. The identification method of modal parameters introduced in the present work gives an instrument to interpret experimental results.

The proposed approach presents some advantages with respect to the metrological methods used to measure gear errors on driving and driven gears [10]; errors are usually measured on only one or few transverse sections of the gears. These metrological methods, which use control machines, provide the charts of profile errors and cumulative pitch and runout errors for each tooth of the two gears (Figure 1). On the other hand, by using the technique presented here, the equivalent error is identified; it is directly related to the gear vibrations and, thus, is particularly appropriate to evaluate the gear accuracy from a dynamic point of view. In fact, it is well known that some modifications of the tooth involute profile can provide a reduction of the vibration level, and hence, the effect of these modifications, in addition to the accuracy of gear profiles and mounting, can be checked by using the equivalent error. The proposed method could be also useful for the condition monitoring of a gear pair.

The effect of noise on the identification of the equivalent error and modal parameters is also investigated. Some simulated tests are performed with noise polluted vibration responses of the gear pair. The method is applied to identify modal parameters and the equivalent error of a gear pair having only profile errors.

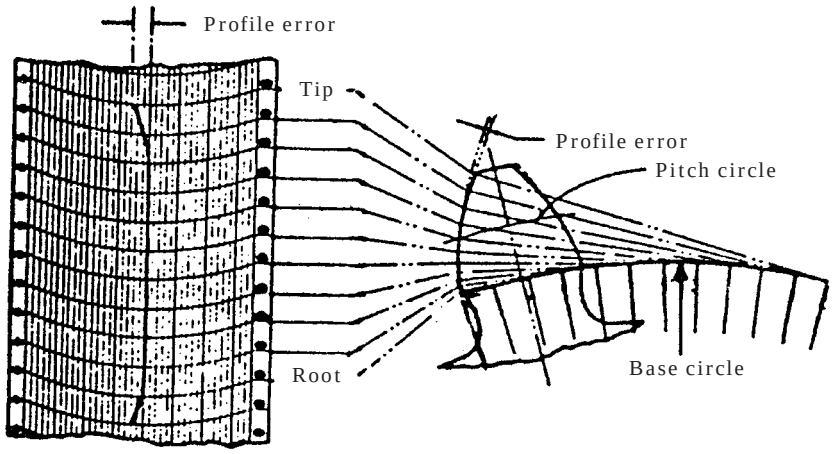

Figure 1. Relation between the profile error chart and the involute tooth profile by reference [15].

2. VIBRATION SIMULATION

A pair of spur gears is modelled with two disks coupled by non-linear mesh stiffness, mesh damping and excitation due to gear errors. One disk (the driving gear) has radius R_1 and the mass moment of inertia of the pinion-shaft system is I_1, while the other (the driven gear) has radius R_2 and the mass moment of inertia of the gear-shaft system is I_2. The radii R_1 and R_2 correspond to the radii of the base circles of the gears 1 and 2, respectively.

The transmission error, defined as the difference between the actual and ideal positions of the driven gear, is expressed as a linear displacement along the line of action. The sign convention used for the transmission error is positive behind the ideal position of the driven gear. Analyzing gears with low contact ratio ε (i.e., $1 < \varepsilon < 2$), the non-linear equation of motion for the dynamic transmission error x can be written as (Figure 2):

$$m\ddot{x} + c\dot{x} + f_1(x, t) + f_2(x, t) = W_0, \tag{1}$$

where

$$x = R_1\theta_1 - R_2\theta_2, \tag{2}$$

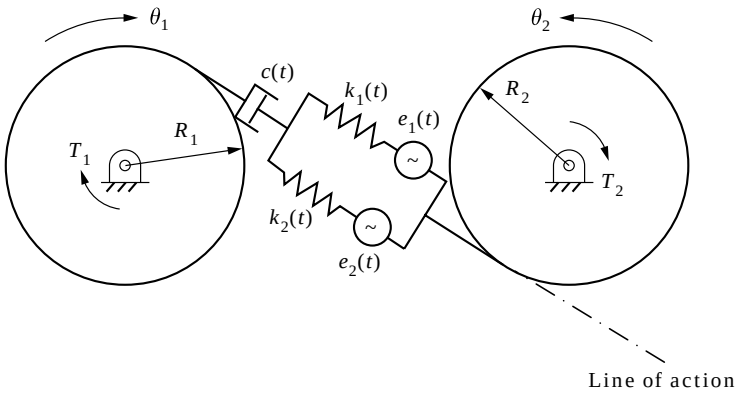

Figure 2. Single-degree-of-freedom model of a pair of spur gears.

θ_1 and θ_2 being the angular displacements of the two gears; the equivalent mass of inertia m of the system is:

$$m = I_1 I_2/(I_1 R_2^2 + I_2 R_1^2); \tag{3}$$

W_0 is the static load given by

$$W_0 = T_1/R_1 = T_2/R_2, \tag{4}$$

T_1 and T_2 being the driving and driven torques, respectively; $f_j(x, t)$ are the elastic forces of the meshing tooth pair j, for $j = 1, 2$

$$f_j(x, t) = \begin{cases} k_j(t)[x - e_j(t)] & \text{when } x - e_j(t) > 0 \\ 0 & \text{when } x - e_j(t) \leqslant 0. \end{cases} \tag{5}$$

Obviously, equation (1) can be easily extended to high contact ratio gears. In equation (5), $k_1(t)$ and $k_2(t)$ are the time-varying meshing stiffnesses of the two pairs of meshing teeth. The error functions $e_1(t)$ and $e_2(t)$ are the displacement excitations along the line of action representing the relative gear errors of the meshing teeth as shown in Figure (2). When two pairs of teeth come into contact there will be two separate error functions, each acting on a different spring. It is assumed that positive error functions give a positive transmission error. Error functions represent the sum of pitch, profile, pressure angle and runout errors. The relation between the flank deviation and the gear errors measured along the line of action is shown in Figure (1). Deviations are assumed to be small enough so that tooth contacts remain on the theoretical line of action [4]. Moreover, from equation (5), the dynamic forces $f_j(x, t)$ become zero when separation of tooth pairs occurs. This is due to the relative vibrations and backlash between the gear teeth; the dynamic forces are the non-linear terms in the equation of motion. In equation (1) a constant viscous damping having coefficient c is assumed.

The total stiffness of the gear pair is given by $k(t) = k_1(t) + k_2(t)$. Introduce the meshing circular frequency $\omega = z\tilde{\Omega}$, where $\tilde{\Omega}$ is the angular velocity of the driven gear (rad/s) and z its number of teeth. The stiffness $k_j(t)$, which is a periodic function, is assumed to have a principal period $T = 2\pi/\omega$. The stiffness is assumed to be independent of the geometrical errors; this hypothesis could be incorrect for lightly loaded gears. The behaviour of $k_j(t)$ and $k(t)$ are discussed in references [3, 6, 10] and in section 4.

In the present paper, the case when $x - e_j(t) > 0$, i.e., when there is contact between the two gears, is considered. Hence, the following study is correct when there is no tooth separation between driving and driven gears. The phenomenon of tooth separation is described in reference [13]. The equation of motion (1) can then be written as a second order linear ordinary differential equation:

$$\ddot{x} + 2\zeta\omega_0\dot{x} + \omega_0^2 K(t)x = F_0 + \omega_0^2 K_1(t)e_1(t) + \omega_0^2 K_2(t)e_2(t), \tag{6}$$

where $K(t) = k(t)/k_m$, $K_1(t) = k_1(t)/k_m$, $K_2(t) = k_2(t)/k_m$, $F_0 = W_0/m$ and $\zeta = c/(2m\omega_0)$ is the damping ratio; K, K_1 and K_2 are non-dimensional functions. Furthermore, the average value of the mesh stiffness is $k_m = (1/T)\int_0^T k(t)\,\mathrm{d}t$ and $\omega_0 = \sqrt{k_m/m}$ is the natural circular frequency of the undamped system with stiffness equal to its integral average value.

It is useful to introduce the following Fourier expansion of the equivalent gear error $v(t)$ [m]

$$v(t) = K_1(t)e_1(t) + K_2(t)e_2(t) = \sum_{n=-\infty}^{\infty} d_n \, e^{in\Omega t}, \tag{7}$$

where i is the imaginary unit and $v(t)$ represents the equivalent error of the gear pair; $v(t)$ is the excitation due to gear errors on the right-side of equation (6). The same tooth of the driving and driven gears mesh together only after a period szT, where s and s_1 are the integers that express the gear ratio τ as the rational number $\tau = s/s_1$ (usually $\tau \leqslant 1$). Therefore, the function $v(t)$ has a principal circular frequency $\Omega = \tilde{\Omega}/s$.

Equation (6) can be used to identify $v(t)$ by quasi-static measurement (loaded transmission error). In fact, for very slow pinion rotational speed, $\ddot{x}$ and $\dot{x}$ can be neglected in equation (6). However, this identification requires very accurate sensors for angular displacement (encoders). In fact, measurement of θ_1 and θ_2 must be very accurate in order to obtain the actual x by using equation (2).

It is interesting to observe that, in many cases, the profile errors can be considered the same for all the gear teeth, i.e., they all have principal period T. Thus, the coefficients d_n for $n = sz, 2sz, 3sz, \ldots$ are due to periodic profile errors, whereas the others are due to pitch and runout errors. In particular, runout errors affect coefficients d_n for $n = s, 2s, 3s, \ldots$ because they have principal period zT. In some cases only the measurement of profile errors is required.

The expansion of the non-dimensional total meshing stiffness is

$$K(t) = \sum_{j=-\infty}^{\infty} \alpha_j \, e^{ijsz\Omega t}. \tag{8}$$

The solution of the equation of motion (6) is obtained by using the harmonic balance method, and the dynamic transmission error x is therefore expanded into a complex Fourier series

$$x(t) = \sum_{n=-\infty}^{\infty} c_n \, e^{in\Omega t}. \tag{9}$$

Substituting equations (7)–(9) into equation (6), results in the following equation:

$$\sum_{n=-\infty}^{\infty} \left[-n^2\Omega^2 c_n + 2in\zeta\omega_0\Omega c_n + \omega_0^2 \sum_{j=-\infty}^{\infty} c_{n-szj}\alpha_j \right] e^{in\Omega t} = F_0 + \omega_0^2 \sum_{n=-\infty}^{\infty} d_n \, e^{in\Omega t}. \tag{10}$$

A simple manipulation of equation (10) produces the following algebraic linear system

$$\mathbf{AC} = \mathbf{F}, \tag{11}$$

where the elements of the matrix $\mathbf{A}$ are given by

$$A_{n,j} = (-n^2\Omega^2 + 2in\zeta\omega_0\Omega)\delta_{n,j} + \omega_0^2\psi_{n,j}\alpha_{(n-j)/(sz)}, \tag{12}$$

where $\delta_{n,j}$ is the Kronecker delta and

$$\psi_{n,j} = \begin{Bmatrix} 1 & \text{if } (n-j)/(sz) \text{ is integer} \\ 0 & \text{otherwise} \end{Bmatrix}$$

and

$$\mathbf{C} = \begin{Bmatrix} c_N \\ \vdots \\ c_1 \\ c_0 \\ c_{-1} \\ \vdots \\ c_{-N} \end{Bmatrix}, \qquad \mathbf{F} = \begin{Bmatrix} \omega_0^2 d_N \\ \vdots \\ \omega_0^2 d_1 \\ F_0 + \omega_0^2 d_0 \\ \omega_0^2 d_{-1} \\ \vdots \\ \omega_0^2 d_{-N} \end{Bmatrix}. \tag{13, 14}$$

3. IDENTIFICATION OF MODAL PARAMETERS AND GEAR ERRORS

The aim of this work is to identify the equivalent gear error; therefore the vector $\mathbf{F}$ in equation (11) is unknown. On the other hand, the contact ratio ε, the shape of the stiffness function $K(t)$ and all the constants α_n of the expansion are known. The transmission error $x(t)$ is then experimentally measured for different rotational speeds $\tilde{\Omega}$ of the driven gear. It is important to note that $\Omega = \tilde{\Omega}/s$, thus either Ω or $\tilde{\Omega}$ can be used as variable. In particular, only rotational speeds where no tooth separation occurs must be chosen. It is obvious that the dynamic transmission error varies according to the speed $\tilde{\Omega}$, so that the coefficients c_n of the expansion and the vector $\mathbf{C}$ are functions of $\tilde{\Omega}$. Equation (12) shows that the matrix $\mathbf{A}$ is also a function of $\tilde{\Omega}$, whereas the vector $\mathbf{F}$ is independent of it. Thus, the equation can be rewritten as:

$$\mathbf{F} = \mathbf{A}(\tilde{\Omega})\mathbf{C}(\tilde{\Omega}). \tag{15}$$

In equation (15), the vector $\mathbf{C}(\tilde{\Omega})$ is obtained experimentally whereas the matrix $\mathbf{A}(\tilde{\Omega})$ is obtained theoretically by using equation (12). However, in order to compute the matrix $\mathbf{A}$, the modal parameters ω_0 and ζ of the system must be identified because they appear in equation (12). These parameters can be determined by using the following equation:

$$\mathbf{A}(\tilde{\Omega}_1)\mathbf{C}(\tilde{\Omega}_1) = \mathbf{A}(\tilde{\Omega}_2)\mathbf{C}(\tilde{\Omega}_2) = \mathbf{A}(\tilde{\Omega}_i)\mathbf{C}(\tilde{\Omega}_i) = \text{constant}, \tag{16}$$

where $\tilde{\Omega}_i$ are fixed rotational speeds. Then,

$$\sum_{n=-\infty}^{\infty} \left[-n^2\Omega^2 c_n + 2in\zeta\omega_0\Omega c_n + \omega_0^2 \sum_{j=-\infty}^{\infty} c_{n-szj}\alpha_j \right] = \text{constant}. \tag{17}$$

By computing the left-side of equation (17) for different rotational speeds, e.g., $\tilde{\Omega}_1$, $\tilde{\Omega}_2$, $\tilde{\Omega}_3$, and subtracting first the quantity computed for $\tilde{\Omega}_2$ from the one computed for $\tilde{\Omega}_1$ followed

by the subtraction of the quantity computed for $\tilde{\Omega}_3$ from the one computed for $\tilde{\Omega}_1$, one obtains the following linear system:

$$\begin{bmatrix} \sum_{n=-\infty}^{\infty} 2ni[(\tilde{\Omega}_1/s)c_n(\tilde{\Omega}_1) - (\tilde{\Omega}_2/s)c_n(\tilde{\Omega}_2)] & \sum_{n=-\infty}^{\infty}\sum_{j=-\infty}^{\infty} \alpha_j[c_{n-szj}(\tilde{\Omega}_1) - c_{n-szj}(\tilde{\Omega}_2)] \\ \sum_{n=-\infty}^{\infty} 2ni[(\tilde{\Omega}_1/s)c_n(\tilde{\Omega}_1) - (\tilde{\Omega}_3/s)c_n(\tilde{\Omega}_3)] & \sum_{n=-\infty}^{\infty}\sum_{j=-\infty}^{\infty} \alpha_j[c_{n-szj}(\tilde{\Omega}_1) - c_{n-szj}(\tilde{\Omega}_3)] \end{bmatrix} \times \begin{Bmatrix} \zeta\omega_0 \\ \omega_0^2 \end{Bmatrix} = \begin{Bmatrix} \sum_{n=-\infty}^{\infty} n^2[(\tilde{\Omega}_1/s)^2 c_n(\tilde{\Omega}_1) - (\tilde{\Omega}_2/s)^2 c_n(\tilde{\Omega}_2)] \\ \sum_{n=-\infty}^{\infty} n^2[(\tilde{\Omega}_1/s)^2 c_n(\tilde{\Omega}_1) - (\tilde{\Omega}_3/s)^2 c_n(\tilde{\Omega}_3)] \end{Bmatrix}. \tag{18}$$

The linear system (18) allows the identification of the modal parameters ω_0 and ζ and, using equation (15), the vector **F** that gives the equivalent gear error. If the quantity $\omega_0^2 d_0$ is negligible with respect to F_0, the ratio W_0/m can also be identified. Hence, if the static load W_0 is known, the reduced mass m of the system is obtained. Actually all the constant terms of the identified vector **F** can be attributed to the static load, making d_0 zero. In fact, the static load can be considered the mean value of the load during the gear meshing and a non-zero coefficient d_0 is equivalent to a change in the static load. For gears with corrected profiles, d_0 can be different from zero; the coefficient $d_0 \neq 0$ can be identified when the static load and the inertia of the gear system are known.

In system (18) one can substitute the quantity $\tilde{\Omega}_2 - \tilde{\Omega}_3$ for one of the two differences previously computed. However, it is important to note that, with measurements at three different speeds, only two linearly independent equations can be obtained for the system (18).

Due to the errors introduced in the experimental measurement of the dynamic transmission error x (errors in **C**), it is preferable to solve an overdetermined system using different velocities to obtain additional equations in system (18). Moreover, the problem is ill-conditioned, so that the errors of the known vector **C** are amplified in the solution. In order to overcome this problem, it is necessary to use only the more significant harmonics in the identification when significant measurement errors or differences between the single-degree-of-freedom model and the actual test bench are observed. Consequently, all the sums involved in system (18) must be stopped at integers n and j which are not too large, since higher order harmonics involved in **C** only introduce noise and do not give additional information. This process is similar to the use of a low-pass filter on signals coming from sensors in experiments. A discussion on this phenomenon is deferred to section 5. The natural circular frequency of the system can also be evaluated theoretically or experimentally and the damping ratio can also be experimentally determined by an impact test, when the system is not rotating, using the logarithmic decrement. The damping ratio can be assumed to vary between 0·07 and 0·1 for some applications, as verified by many authors, e.g., references [6, 10]. The results of the identification can therefore be compared with data obtained in a different way.

The vector **F** can be determined by using equation (15) or the following expression:

$$\mathbf{F} = (1/I)\sum_{i=1}^{I} \mathbf{A}(\tilde{\Omega}_i)\mathbf{C}(\tilde{\Omega}_i). \tag{19}$$

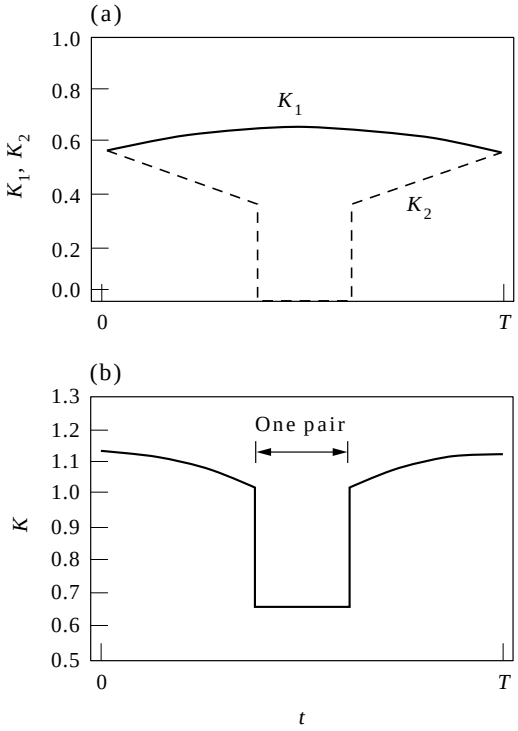

Figure 3. (a) The non-dimensional meshing stiffnesses $K_1(t)$ and $K_2(t)$. (b) The total meshing stiffness $K(t)$.

This procedure provides a good accuracy in the computation in the presence of measurement errors. The average introduced in equation (19) reduces the errors introduced in the experimental measurement of x (and consequently in $\mathbf{C}$). Furthermore, in this case it could be useful to avoid high harmonics, because a very high noise level undoubtedly affects them.

4. APPLICATION OF THE METHOD

In order to apply the proposed method, a function describing the stiffness of the gear pair must be determined. In the paper of Umezawa *et al*. [10], seven different stiffness functions are discussed; differences between these functions are mainly due to a different simulation of the behaviour of the stiffness in the region where there is the interference of the tip of tooth (called tooth tip meshing).

The stiffness function proposed by Cai and Hayashi [6] was used in the numerical simulations performed in the present study. This formula depends only on the contact ratio ε and is independent of the transmitted torque. Obviously, the proposed method can be used with different expressions of the meshing stiffness. In particular, the following function is introduced:

$$f(t) = \frac{1}{0{\cdot}85\varepsilon}\left[\frac{-1{\cdot}8}{(\varepsilon T)^2}[t + ((\varepsilon - 1)/2)T]^2 + \frac{1{\cdot}8}{\varepsilon T}[t + ((\varepsilon - 1)/2)T] + 0{\cdot}55\right]. \tag{20}$$

The two non-dimensional meshing stiffnesses $K_1(t)$ and $K_2(t)$ are directly obtained from equation (20)

$$K_1(t) = f(t) \quad \text{for} \quad 0 \leqslant t \leqslant T, \tag{21}$$

$$K_2(t) = \begin{Bmatrix} f(t-T) & \text{if } t > T - ((\varepsilon-1)/2)T \\ 0 & \text{if } t \leqslant T - ((\varepsilon-1)/2)T \end{Bmatrix} + \begin{Bmatrix} f(t+T) & \text{if } t < ((\varepsilon-1)/2)T \\ 0 & \text{if } t \geqslant ((\varepsilon-1)/2)T \end{Bmatrix}$$

$$\text{for} \quad 0 \leqslant t \leqslant T. \tag{22}$$

The two non-dimensional meshing stiffnesses $K_1(t)$ and $K_2(t)$ are shown in Figure 3(a) ($\varepsilon = 1{\cdot}8$) along the meshing period $T = 2\pi/\omega$, and the non-dimensional total meshing stiffness $K(t)$ is plotted in Figure 3(b). The integral average stiffness of the pair k_m is related to the maximum stiffness of one pair of teeth k_{MAX} by the following expression: $k_m = 0{\cdot}85\varepsilon k_{MAX}$. The ISO/DIS 6336-1.2 (1990) design code gives a formula to evaluate k_{MAX}.

In order to simplify the experimental measurement of the dynamic transmission error, sometimes measurement on only one gear is performed. Usually the acceleration of the driven gear $\ddot{x}_2 = R_2\ddot{\theta}_2$ is measured; however, the acceleration $\ddot{x}$ can be obtained by using the following relationship:

$$\ddot{x}_2 = \frac{m_1\ddot{x} + F_1(t) - F_2(t)}{m_1 + m_2}, \tag{23}$$

where $m_1 = I_1/R_1^2$ and $m_2 = I_2/R_2^2$ are the reduced masses of the driving gear–shaft and the driven gear–shaft system and F_1 and F_2 are the forces acting on the driving and driven gears as a consequence of the driving and driven torques T_1 and T_2, respectively. Using m_1 and m_2, the equivalent inertia mass m of the system, equation (3), is $m = (m_1m_2)/(m_1 + m_2)$. It is to note that forces F_1 and F_2 are not necessarily equal in dynamic conditions. Their difference generates a movement of the centre of mass of the two masses' system m_1 and m_2. However, if a good motor and brake are used and torsionally compliant joints are interposed in the connection of the motor and brake to the gears, the difference between forces F_1 and F_2 can be neglected with respect to $m_1\ddot{x}$. In fact, oscillations of the centre of mass of the system m_1 and m_2 are considered to have a natural frequency (due to joint flexibility) much lower (and therefore uncoupled) than the natural meshing frequency and rotational speed. A filter can eliminate this low-frequency effect due to forces F_1 and F_2.

The measured acceleration can be related to coefficients c_n by equation (9) to yield:

$$\ddot{x}_2 = -\frac{m_1}{m_1 + m_2}\Omega^2 \sum_{n=-\infty}^{\infty} c_n n^2 \, \mathrm{e}^{\mathrm{i}n\Omega t}. \tag{24}$$

Equation (24) shows that the coefficient c_0 cannot be obtained by vibration measurement. However, this coefficient can easily be determined because it is the mean value of the dynamic transmission error x. A good estimation of this value is $c_0 = W_0/k_m$ for gears with ideal involute profile, while Munro [29] has shown that for spur gears with symmetric long relief $c_0 = W_0/k_{minimum}$ under specific conditions. In the identification process it is very important to only use measured accelerations when no teeth separation occurs. Thus, it is generally necessary to avoid rotational speeds larger than half the main resonance speed ω_0. It is also important to synchronize the stiffness functions with the measured response.

In the past some experimental apparatus were designed to measure the dynamic transmission errors of spur gear pairs. Usually, they are assembled in order to minimize the bending of the shafts and the deflection of bearings. Gregory *et al*. [33, 34] described

the experiments performed by Munro on a "four-square test rig" that has a test gear pair and a slave gear pair for power recirculation. Another apparatus was built by Umezawa *et al*. [10] without power recirculation. Both the apparatus showed the effect of bearings vibration on the measured dynamic response. More recently, Cai and Hayashi [6] used high stiffness air bearings in order to minimize the effects of bearings. Another sophisticated test rig with power recirculation was assembled by Blankenship and Kahraman [30, 31]. They used oversized ultra-precision spherical roller bearings which are themselves supported by rigid bearings pedestals; they obtained results according to a single-degree-of-freedom model. This recent trend of research is in the direction of experimental apparatus that have more and more the characteristics required by our identification method.

Based on the cited papers, the benchmark for gears can be obtained by a variable speed motor and a brake, or can be the "four-square test rig" that has a test gear pair and a slave gear pair for power recirculation [30, 31]. Stiff shafts in bending and torsion, compliant elastomeric couplings with very low natural frequency, and stiff bearings must be used in order to approximate well a single-degree-of-freedom system. The rotational speed can be measured by a proximity sensor that counts the number of passing teeth and can be used also as a synchronizer; the load is measured by a dynamometer and the acceleration of the driven gear by accelerometers. A slip ring is introduced to bring the signals to the amplifier. Alternatively, a laser rotational vibrometer can be employed to

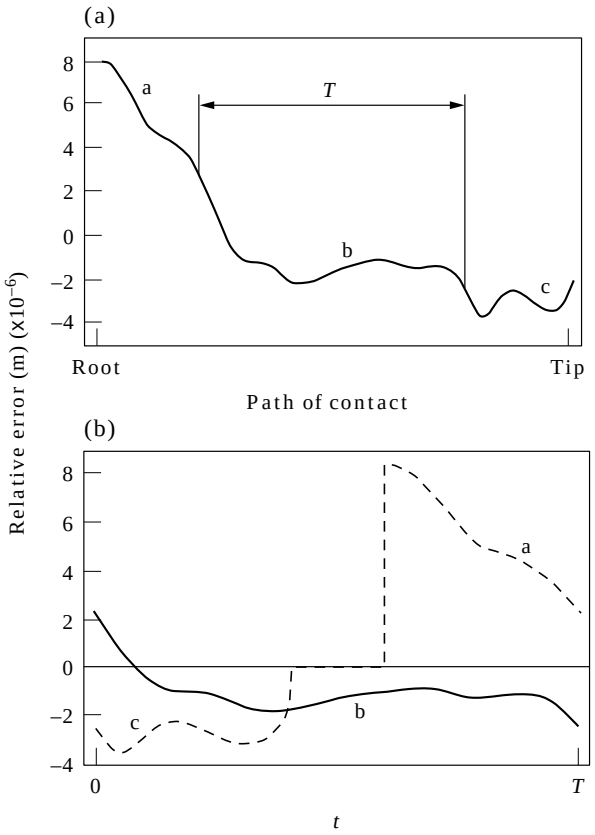

Figure 4. Profile errors of the studied gear pair. (a) Relative gear errors obtained by data reported in reference [10]. (b) Error functions e_1 (——), and e_2 (—·—).

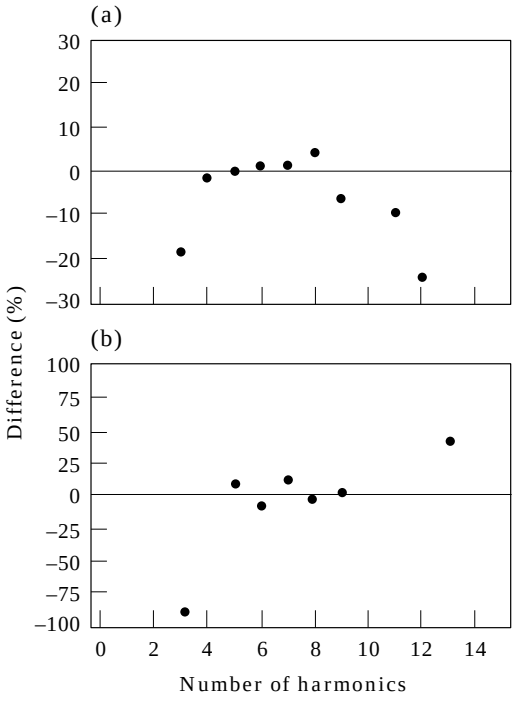

Figure 5. Results of the identification with an error level $lev = 0{\cdot}02$. (a) Percentage difference between the identified ω_0 and the actual value versus the number of harmonics used in the identification. (b) Percentage difference between the identified ζ and the actual value versus the number of harmonics.

measure vibrations of the driven gear; in this case accelerometers, slip ring and summing amplifier can be eliminated.

5. NUMERICAL RESULTS

To verify the proposed method, the gear pair tested by Umezawa *et al*. [10] is studied. The two gears are finished by a MAAG grinding. The characteristics of both gears are: module = 4, number of teeth = 48, face width = 10 mm, pressure angle = $14{\cdot}5^\circ$, diameter of standard pitch circle = 192 mm and gear ratio = 1. The natural circular frequency is $\omega_0 = 48 \times 3062$ r.p.m. (2450 Hz) and the damping ratio $\zeta = 0{\cdot}07$. The contact ratio ε is 1·8, the rotational speed range $\tilde{\Omega} = 400 \leftrightarrow 3000$ r.p.m. ($41{\cdot}89 \leftrightarrow 314{\cdot}16$ rad/s), the torque = 196 Nm and the teeth have an involute profile. It is assumed that only profile errors are significant in this case, hence, all the other errors are neglected. As a consequence of this hypothesis, the dynamic transmission error has a principal period equal to the meshing period T. The profile errors are approximately 6 μm at the root of the driving gear and at the tip of the driven gear; these profile errors are reported in reference [10] for one transverse section. The relative error (sum of errors on the driving and driven gears) of a tooth pair of this gear system is reported in Figure 4(a) for the whole path of contact. The gear errors functions e_1 and e_2 are directly obtained by the procedure graphically shown in Figure 4. In particular, the relative error of Figure 4(a) is divided into three parts; part "b" corresponds to the central arc of temporal length T, while the entire contact length of a pair of teeth is εT. The three parts are arranged as shown in Figure 4(b) in order to obtain the two error functions e_1 and e_2.

In reference [10], as well as in other papers, few experimentally measured responses of rotational vibration are reported. As a consequence, it was preferred to use responses theoretically computed for the gear pair studied in reference [10]. Hence, all the accelerations used in the following part of this section were simulated; only in section 5.1 are experimental data used to identify the equivalent error.

The computed responses of the gear pair are polluted with noise. In particular, the response x is discretized with 201 points in the period T and the noise is then added to the response before computing the vector $\mathbf{C}$. The noise is generated using random numbers added to the time response. These random numbers are obtained by a normal distribution having zero mean value and variance $\sigma = lev \cdot max$, where max is the maximum value of the response x in the period and lev is the error level. As a consequence of the assumed distribution, 68% of the points have noise within $\pm\sigma$, 95% within $\pm 2\sigma$ and 99·7% within $\pm 3\sigma$.

First, equation (18) is used to identify the modal parameters of the system from noise polluted responses. In particular eight responses at rotational speeds $\tilde{\Omega} = 60$, 65, 68, 70, 80, 90, 100, 120 rad/s with an error level $lev = 0{\cdot}02$ are employed. This error level gives responses having a difference within $\pm 6\%$ of the maximum value (for 99·7% of points) with respect to the true value. In Figure 5(a) the percentage difference between the identified natural frequency ω_0 and the actual value is plotted versus the number of harmonics of both the meshing stiffness and the vibration responses used in the identification, equation (18). The range of harmonics of the meshing frequency $\omega = z\tilde{\Omega}$ that gives correct results is $4 \leqslant n = j \leqslant 8$. In Figure 5(b) the data relative to the damping ratio ζ are reported. Figure 6 is similar to Figure 5 but is obtained for an increased error level $lev = 0{\cdot}04$ (noise within $\pm 12\%$ of the maximum value). In this case, the range of

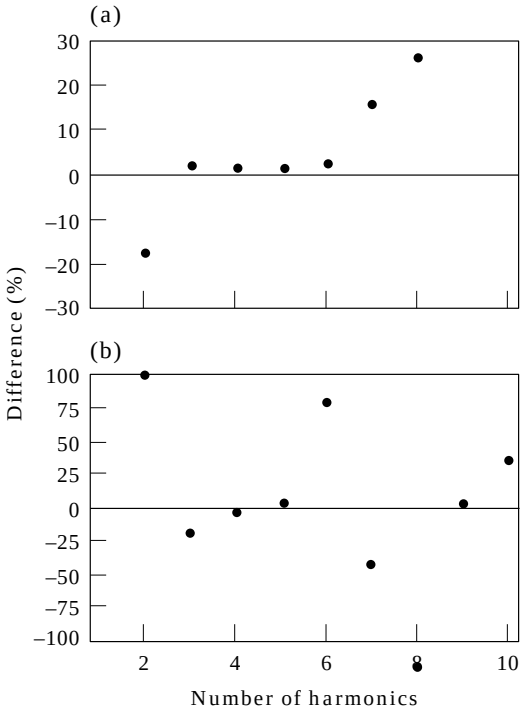

Figure 6. Results of the identification with an error level $lev = 0{\cdot}04$. (a) Percentage difference between the identified ω_0 and the actual value. (b) Percentage difference between the identified ζ and the actual value.

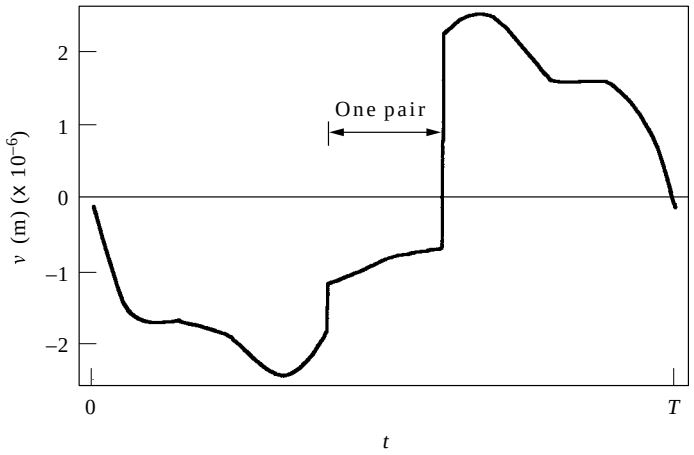

Figure 7. Actual equivalent gear error $v(t)$ for the studied gear pair.

useful harmonics decreases. Note that this error level is quite large. Figures 5 and 6 show that increasing largely the number of harmonics is not convenient. In fact, for the problem considered, the amplitude of coefficients c_n decreases with n so that higher order harmonics are largely affected by the noise. The identification process being an ill-conditioned problem, it is necessary to employ only harmonics having a good signal to noise ratio.

The identification process gives both the natural frequency ω_0 and the damping ratio ζ of the rotating gear pair. It was verified numerically that identification of these modal parameters at rotational speeds below the secondary resonance gives more accurate results. In fact, in this case, the larger harmonic of the response has at least two waves, hence, a good signal to noise ratio was obtained for the first harmonics.

In Figure 7, the equivalent error obtained by using the profile errors reported in Figure 4 and in reference [10] is shown; this can be called the "actual" equivalent error.

The equivalent error is identified in Figure 8 by using a response at $\tilde{\Omega} = 60$ rad/s without noise and equation (15). In this case, 15 harmonics are used to describe the function. The difference between Figures 7 and 8 can definitively be attributed to the truncation error.

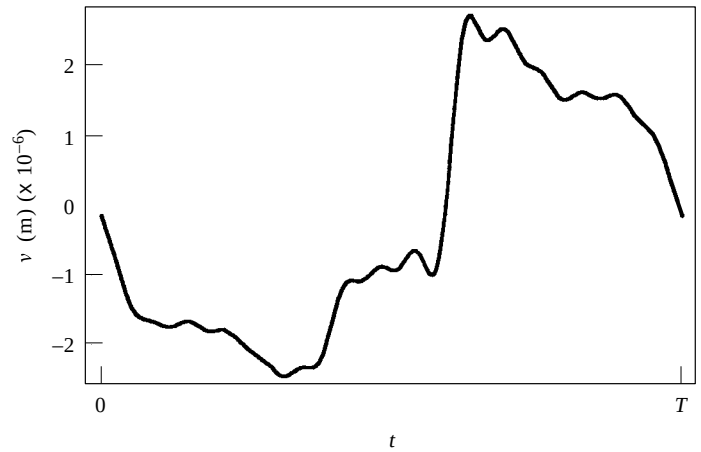

Figure 8. Identified equivalent gear error by response without noise.

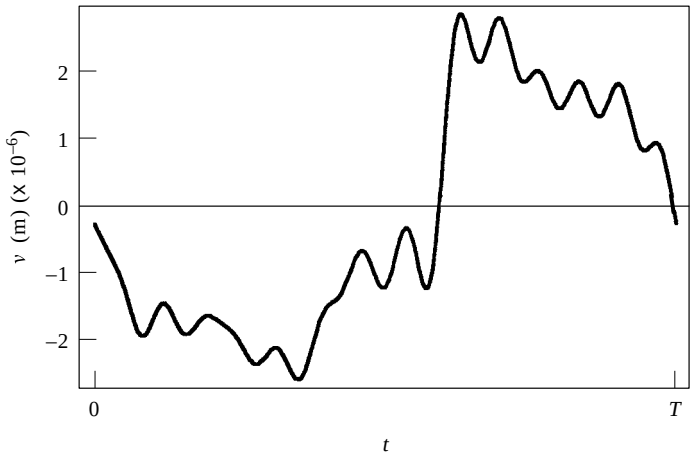

Figure 9. Identified equivalent gear error by responses with a noise level $lev = 0{\cdot}02$; actual modal parameters.

Eight responses at rotational speeds $\tilde{\Omega} = 60, 65, 68, 70, 80, 90, 100, 120$ rad/s polluted with an error (noise) level $lev = 0{\cdot}02$ (error $\pm 6\%$) are then used to identify the equivalent error. In this case equation (19) is utilized. The result is given in Figure 9, where the actual modal parameters (ω_0 and ζ) are used. Figures 8 and 9 are very similar and they describe well the "actual" error reported in Figure 7. The effect of an incorrect identification of the modal parameters ω_0 and ζ on the evaluation of the equivalent gear error is then investigated in Figure 10. In this case, an error of $+10\%$ on the frequency and $+40\%$ on the damping ratio is used to evaluate the equivalent error by polluted responses having a noise level $lev = 0{\cdot}02$. A reasonably correct result is also obtained.

The case of a noise level $lev = 0{\cdot}04$ (error $\pm 12\%$), combined with the use of an error of $+10\%$ on the frequency and $+40\%$ on the damping ratio, is studied in Figure 11. A fairly good evaluation of the equivalent error is also reached in this case, where only the first ten harmonics of the responses and mesh stiffness are used. In fact, this figure presents less high-frequency noise than Figures 9 and 10.

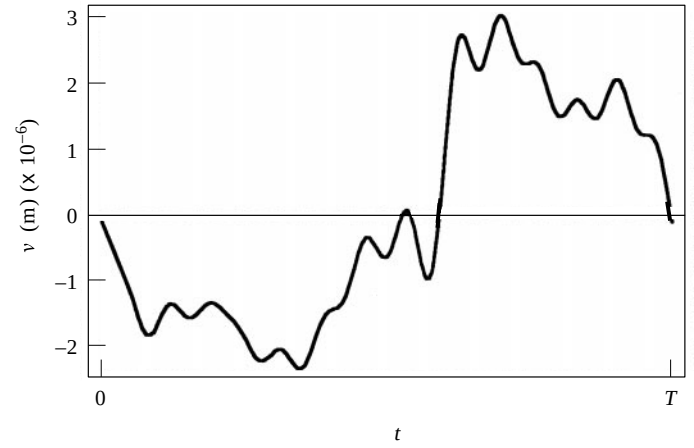

Figure 10. Identified equivalent gear error by responses with a noise level $lev = 0{\cdot}02$; $+10\%$ of the actual value on ω_0 and $+40\%$ on the actual value of ζ.

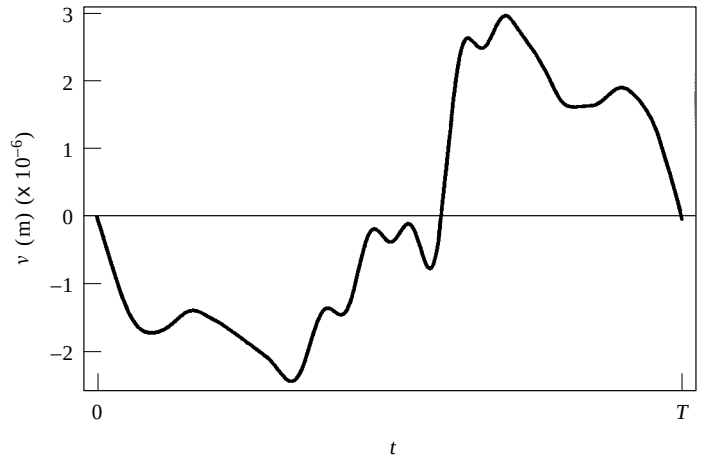

Figure 11. Identified equivalent gear error by responses with a noise level $lev = 0{\cdot}04$; $+10\%$ of the actual value on ω_0 and $+40\%$ on the actual value of ζ.

5.1. IDENTIFICATION BY EXPERIMENTAL DATA

The experimental acceleration of the studied gear pair is only available in reference [10] with a reasonably accurate figure at a rotational speed of 1200 r.p.m. The acceleration was measured on the driven gear and is shown in Figure 12, where it is synchronized with respect to the stiffnesses K_1, K_2 and K reported in Figures 3(a) and (b). Thus, the acceleration relative to a single pair of teeth in contact is in the central part of Figure 12. The equivalent error is then identified by using this experimental result and is shown in Figure 13. This was done by expanding the acceleration of Figure 12 into the Fourier series given in equation (9). The time origin is the same as in Figure 12, in order to have the acceleration relative to a single pair of teeth in contact in the central part of period T (as done for K). Thus, Figure 13 was obtained by using equation (15), where vector $\mathbf{C}$ contains the Fourier coefficients of the experimental acceleration, as previously described. Note that this acceleration is affected by the vibration of the bearings, as a consequence of the test rig used. This problem is well described in reference [10]. Therefore the identified equivalent

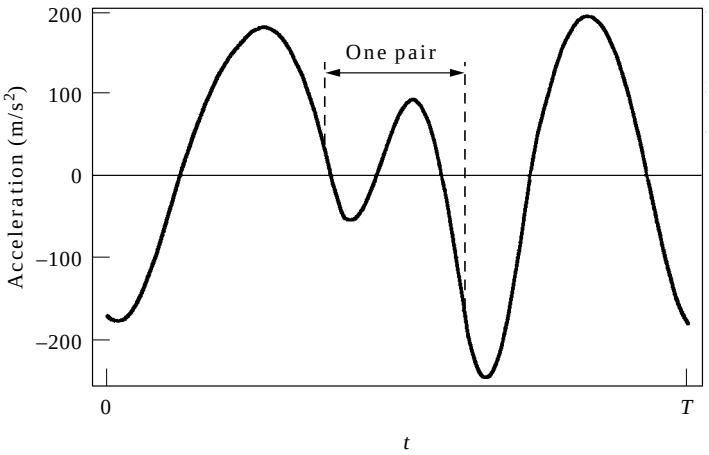

Figure 12. Measured acceleration on the driven gear of the studied gear pair reported in reference [10] at 1200 r.p.m.

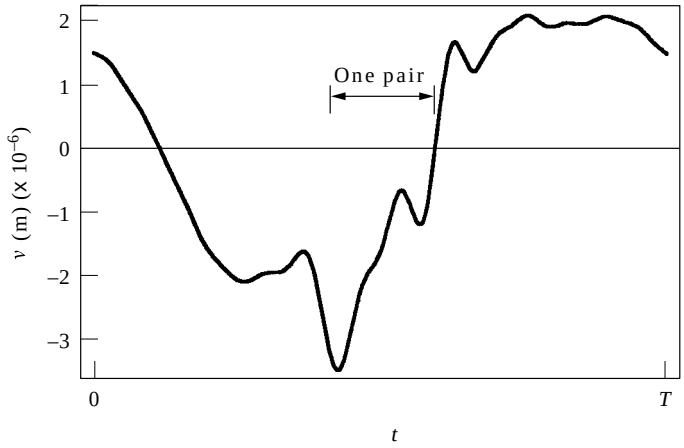

Figure 13. Identified equivalent gear error by using the experimental acceleration at 1200 r.p.m.

error is not so close to the "actual" one. In this case, it was not possible to identify the modal parameters using equation (18) and the equivalent error was therefore obtained by equation (15) due to the few data available in reference [10]. Furthermore, the "actual" equivalent gear error, Figure 7, was obtained by using metrological gear errors measured on only one transverse section of the gears. Hence, the effective behaviour of the gear pair is different from the one simulated. Lastly, it is interesting to note that the equivalent gear error shown in Figure 13 gives a significant reduction of the vibration amplitude with respect to an ideal involute profile of all the teeth of the gear pair.

6. CONCLUSIONS

The proposed method gives a powerful instrument for the identification of the natural frequency and damping of a gear pair tested in working conditions. In fact, determination of modal parameters of a gear pair is still far from being considered as well established. The reconstruction of the equivalent gear error by acceleration measurement of the driven gear of a spur gear pair is also reasonably good in the case of data affected by noise. In particular the identification of the natural frequency and damping of the system is obtained by an overdetermined linear system to minimize the error; to obtain correct results only lower order harmonics must be considered. Then, this data can be used to evaluate the equivalent gear error that is not largely affected by the inaccuracy in the identification of the natural frequency and damping.

The proposed method seems to have advantages in the quality control of a large production of gears having the same centre distance; in this case the same housing can be used. The gear can be tested together with a reference gear or with the companion gear to check the actual gear pair. Moreover the method could be useful for the condition monitoring of a gear pair. As a limitation, it can only be applied to systems having stiff bearings and torsionally compliant axes, requiring an appropriately designed test bench.

The identified equivalent gear error does not present the problem of metrological data that are usually obtained on only one or few transverse sections of the gears. On the contrary, it describes the global behaviour of the pair, similar to quasi-static transmission error measurements.

ACKNOWLEDGMENT

The authors gratefully acknowledge the referees who helped them to improve the original work.

REFERENCES

1. H. N. Özgüven and D. R. Houser 1988 *Journal of Sound and Vibration* **121**, 383–411. Mathematical models used in gear dynamics.
2. H. N. Özgüven and D. R. Houser 1988 *Journal of Sound and Vibration* **125**, 71–83. Dynamic analysis of high speed gears by using loaded static transmission error.
3. M. Amabili and A. Rivola 1997 *Mechanical Systems and Signal Processing* **11**, 375–390. Dynamic analysis of spur gear pairs: steady state response and stability of the SDOF model with time-varying meshing stiffness.
4. P. Velex and M. Maatar 1996 *Journal of Sound and Vibration* **191**, 629–660. A mathematical model for analyzing the influence of shape deviations and mounting errors on gear dynamic behaviour.
5. Y. Cai and T. Hayashi 1992 *Proceedings of the ASME International Power Transmission and Gearing Conference*, *Scottsdale*, *Arizona* **2**, 453–460 (DE-Vol. 43-2). The optimum modification of tooth profile for a pair of spur gears to make its rotational vibration equal zero. Also published as: Y. Cai and T. Hayashi 1991 *Transactions of the Japan Society of Mechanical Engineers C* **57**, 3957–3963. The optimum modification of tooth profile of power transmission spur gears to make the rotational vibration equal zero (in Japanese).
6. Y. Cai and T. Hayashi 1994 *Transactions of the American Society of Mechanical Engineers*, *Journal of Mechanical Design* **116**, 558–564. The linear approximated equation of vibration of a pair of spur gears (theory and experiment).
7. Y. Cai 1995 *Transactions of the American Society of Mechanical Engineers*, *Journal of Mechanical Design* **117**, 460–469. Simulation on the rotational vibration of helical gears in consideration of the tooth separation phenomenon (a new stiffness function of helical involute tooth pair).
8. Y. Cai 1996 *Proceedings of the ASME International Power Transmission and Gearing Conference*, *San Diego*, *CA*, 177–184 (DE-Vol. 88). Development of a silent helical gear reducer (vibration simulation and noise measurement).
9. T. Sato, K. Umezawa and J. Ishikawa 1983 *Bulletin of the Japan Society of Mechanical Engineers* **26**, 2010–2016. Effects of contact ratio and profile correction on gear rotational vibration.
10. K. Umezawa, T. Sato and J. Ishikawa 1984 *Bulletin of the Japan Society of Mechanical Engineers* **27**, 102–109. Simulation on rotational vibration of spur gears.
11. K. Umezawa, T. Sato and K. Kohno 1984 *Bulletin of the Japan Society of Mechanical Engineers* **27**, 569–575. Influence of gear error on rotational vibration of power transmission spur gears (1st report, pressure angle error and normal pitch error).
12. K. Umezawa and T. Sato 1985 *Bulletin of the Japan Society of Mechanical Engineers* **28**, 2143–2148. Influence of gear error on rotational vibration of power transmission spur gears (2nd report, wave form error).
13. K. Umezawa, T. Ajima and H. Houjoh 1986 *Bulletin of the Japan Society of Mechanical Engineers* **29**, 950–957. Vibration of three axes gear system.
14. A. Kubo, S. Kiyono and M. Fujino 1986 *Bulletin of the Japan Society of Mechanical Engineers* **29**, 4424–4429. On analysis and prediction of machine vibration caused by gear meshing (1st report, nature of gear vibration and the total vibrational excitation).
15. R. Kasuba and J. W. Evans 1981 *Transactions of the American Society of Mechanical Engineers*, *Journal of Mechanical Design* **103**, 398–409. An extended model for determining dynamic loads in spur gearing.
16. W. D. Mark 1987 *Transactions of the American Society of Mechanical Engineers*, *Journal of Mechanisms*, *Transmissions*, *and Automation in Design* **109**, 268–274. Analytical reconstruction of the running surfaces of gear teeth. Part 2: combining tooth spacing measurements with profile and lead measurements.
17. M. Benton and A. Seireg 1978 *Transactions of the American Society of Mechanical Engineers*, *Journal of Mechanical Design* **100**, 26–32. Simulation of resonances and instability conditions in pinion-gear systems.

18. R. W. Cornell and W. W. Westervelt 1978 *Transactions of the American Society of Mechanical Engineers*, *Journal of Mechanical Design* **100**, 69–76. Dynamic tooth loads and stressing for high contact ratio spur gears.
19. W. D. Mark 1978 *Journal of the Acoustical Society of America* **63**, 1409–1430. Analysis of the vibratory excitation of gear systems: basic theory.
20. W. D. Mark 1979 *Journal of the Acoustical Society of America* **66**, 1758–1787. Analysis of the vibratory excitation of gear systems. II: Tooth error representations, approximations, and applications.
21. B. M. Bahgat, M. O. M. Osman and T. S. Sankar 1983 *Transactions of the American Society of Mechanical Engineers*, *Journal of Mechanisms*, *Transmissions*, *and Automation in Design* **105**, 302–309. On the spur–gear dynamic tooth-load under consideration of system elasticity and tooth involute profile.
22. A. S. Kumar, T. S. Sankar and M. O. M. Osman 1985 *Transactions of the American Society of Mechanical Engineers*, *Journal of Mechanisms*, *Transmissions*, *and Automation in Design* **107**, 54–60. On dynamic tooth load and stability of a spur–gear system using the state–space approach.
23. D. C. H. Yang and Z. S. Sun 1985 *Transactions of the American Society of Mechanical Engineers*, *Journal of Mechanisms*, *Transmissions*, *and Automation in Design* **107**, 529–535. A rotary model for spur gears dynamics.
24. D. C. H. Yang and J. Y. Lin 1987 *Transactions of the American Society of Mechanical Engineers*, *Journal of Mechanisms*, *Transmissions*, *and Automation in Design* **109**, 189–196. Hertzian damping, tooth friction and bending elasticity in gear impact dynamics.
25. H.-H. Lin, R. L. Huston and J. J. Coy 1988 *Transactions of the American Society of Mechanical Engineers*, *Journal of Mechanisms*, *Transmissions*, *and Automation in Design* **110**, 221–225. On the dynamic loads in parallel shaft transmissions: Part I—modelling and analysis.
26. H.-H. Lin, R. L. Huston and J. J. Coy 1988 *Transactions of the American Society of Mechanical Engineers*, *Journal of Mechanisms*, *Transmissions*, *and Automation in Design* **110**, 226–229. On the dynamic loads in parallel shaft transmissions: Part II—parameter study.
27. H. N. Özgüven 1991 *Journal of Sound and Vibration* **145**, 239–260. A non-linear mathematical model for dynamic analysis of spur gears including shaft and bearing dynamics.
28. Ö. S. Sener and H. N. Özgüven 1993 *Journal of Sound and Vibration* **166**, 539–556. Dynamic analysis of geared shaft systems by using a continuous system model.
29. R. G. Munro 1991 *Proceedings of the* 1*st IMechE International Conference on Gearbox Noise and Vibration*, *Cambridge*, *UK*, 3–10. A review of the theory and measurement of gear transmission error.
30. G. W. Blankenship and A. Kahraman 1995 *Journal of Sound and Vibration* **185**, 743–765. Steady state forced response of a mechanical oscillator with combined parametric excitation and clearance type non-linearity.
31. G. W. Blankenship and A. Kahraman 1996 *Proceedings of the ASME International Power Transmission and Gearing Conference*, *San Diego*, *CA*, 373–380 (DE-Vol. 88). Gear dynamics experiments, Part I: characterization of forced response.
32. A. H. Nayfeh and D. T. Mook 1979 *Nonlinear Oscillations*. New York: John Wiley and Sons.
33. R. W. Gregory, S. L. Harris and R. G. Munro 1963 *Proceedings of the Institution of Mechanical Engineers* **178**, 166–173. Torsional motion of a pair of spur gears.
34. R. W. Gregory, S. L. Harris and R. G. Munro 1963–64 *Proceedings of the Institution of Mechanical Engineers* **178**, 207–226 (including discussion). Dynamic behaviour of spur gears.

APPENDIX: NOMENCLATURE

c damping coefficient (N s/m)
$\mathbf{C}$ vector of Fourier coefficients of x
e_1 error function of gear 1 (m)
e_2 error function of gear 2 (m)
$\mathbf{F}$ vector of gear error coefficients
F_0 $= W_0/m$, (m/s^2)
I_1 mass moment of inertia of pinion–shaft (kg m^2)
I_2 mass moment of inertia of gear–shaft (kg m^2)
k $= k_1 + k_2$, total meshing stiffness (N/m)
k_1 stiffness of first pair of meshing teeth (N/m)

k_2 stiffness of second pair of meshing teeth (N/m)
k_m integral average of mesh stiffness (N/m)
K $= k/k_m = K_1 + K_2$
K_1 $= k_1/k_m$
K_2 $= k_2/k_m$
lev noise level
m equivalent mass of gear system (kg)
m_1 equivalent mass of gear 1 (kg)
m_2 equivalent mass of gear 2 (kg)
R_1 radius of base circle of gear 1 (m)
R_2 radius of base circle of gear 2 (m)
t time (s)
T meshing principal period (s)
T_1 driving torque (N m)
T_2 driven torque (N m)
W_0 static load (N)
x dynamic transmission error (m)
z number of teeth of driven gear
ε contact ratio
v equivalent error of gear pair (m)
θ_1 angular displacement of gear 1 (rad)
θ_2 angular displacement of gear 2 (rad)
ω meshing circular frequency (rad/s)
ω_0 $= \sqrt{k_m/m}$, natural circular frequency (rad/s)
$\tilde{\Omega}$ angular velocity of driven gear (rad/s)
ζ $= c/(2m\omega_0)$, damping ratio